Modeling glacier extents and equilibrium line altitudes in the Rwenzori Mountains, Uganda, over the last 31,000 yr

Alice M. Doughty* Meredith A. Kelly

Department of Earth Sciences, Dartmouth College, HB6105 Fairchild Hall, Hanover, New Hampshire 03755, USA

James M. Russell

Department of Earth, Environmental, and Planetary Sciences, Brown University, Providence, Rhode Island 02912, USA

Margaret S. Jackson

Department of Earth Sciences, Dartmouth College, HB6105 Fairchild Hall, Hanover, New Hampshire 03755, USA

Brian M. Anderson

Antarctic Research Centre, Victoria University of Wellington, P.O. Box 600, Wellington 6140, New Zealand

Jonathan Chipman

Department of Earth Sciences, Dartmouth College, HB6105 Fairchild Hall, Hanover, New Hampshire 03755, USA

Bob Nakileza

Mountain Resource Centre, Makerere University, Kampala, Uganda

Sylvia G. Dee

Department of Earth, Environmental, and Planetary Sciences, Rice University, Houston, Texas 77005, USA

ABSTRACT

Mountain glacier moraine sequences and their chronologies allow us to evaluate the timing and climate conditions that underpin changes in the equilibrium line altitudes (ELAs), which can provide valuable information on the paleoclimatology of understudied regions such as tropical East Africa. However, moraine sequences are inherently discontinuous, and the precise climate conditions that they represent can be ambiguous due to the sensitivity of mountain glaciers to temperature, precipitation, and other environmental variables. Here, we used a two-dimensional (2-D) iceflow and mass-balance model to simulate glacier extents and ELAs in the Rwenzori Mountains in East Africa over the past 31,000 yr (31 k.y.), including the Last Glacial Maximum (LGM), late glacial period, and the Holocene Epoch. We drove the glacier

^{*}alice.doughty@maine.edu

model with two independent, continuous temperature reconstructions to simulate possible glacier length changes through time. Model input paleoclimate values came from branched glycerol dialkyl glycerol tetraether (brGDGT) temperature reconstructions from alpine lakes on Mount Kenya for the last ~31 k.y., and precipitation reconstructions for the LGM came from various East African locations. We then compared the simulated fluctuations with the positions and ages (where known) of the Rwenzori moraines. The simulated glacier extents reached within 1.1 km of the dated LGM moraines in one valley (93% of the full LGM extent) when forced by the brGDGT temperature reconstructions (maximum cooling of 6.1 °C) and a decrease in precipitation (-10% than modern amounts). These simulations suggest that the Rwenzori glaciers required a cooling of at least 6.1 °C to reach the dated LGM moraines. Based on the model output, we predict an age of 12–11 ka for moraines located halfway between the LGM and modern glacier extents. We also predict ice-free conditions in the Rwenzori Mountains for most of the early to middle Holocene, followed by a late Holocene glacier readvance within the last 2000 yr.

INTRODUCTION

A principal aim of glacial geology is to quantify changes in climate relative to modern conditions. Moraines from mountain glaciers represent past glacier extents and are used to reconstruct equilibrium line altitudes (ELAs), which approximate past climate changes (e.g., Porter, 1975, 2000; Benn et al., 2005; Xu et al., 2010; Sagredo et al., 2014). Moraines relating or dating to the Last Glacial Maximum (LGM, ca. 26.5–19 ka), late glacial (ca. 15-11.7 ka), and Holocene (ca. 11.7-0 calibrated [cal] k.y. B.P.; Clark et al., 2009; Walker et al., 2012) times are of particular interest because they can be identified at most latitudes (e.g., Gosse et al., 1995; Thackray et al., 2004; Briner et al., 2005; Farber et al., 2005; Marchetti et al., 2005; Schaefer et al., 2006, 2009; Briner and Kaufman, 2008; Licciardi and Pierce, 2008; Zech et al., 2009; Kaplan et al., 2010, 2013; Putnam et al., 2010, 2013; Bromley et al., 2011; Kelly et al., 2012, 2014; Jomelli et al., 2014; Kelley et al., 2014; Stroup et al., 2014; Doughty et al., 2015; Bromley et al., 2016; Sagredo et al., 2018), revealing large-scale paleoclimate conditions. For example, reconstructions of glacier extents during the LGM suggest a nearly uniform decrease in ELAs of ~900-1000 m across all latitudes (Porter, 1975; Broecker and Denton, 1990; Porter, 2000). However, the estimates of tropical glacier ELAs during the LGM vary by up to 500 m (Mark et al., 2005), suggesting considerable uncertainty in tropical climate conditions.

The variability in tropical ELA estimates may arise from a number of sources of uncertainty, including uncertainties in moraine ages, local glacier dynamics, and the locally variable combinations of temperature, precipitation, and other environmental variables that influence glacier mass balance. Many tropical ELA reconstructions are derived from moraines with little age control, including moraine sequences for which ages are assumed rather than measured (Porter, 2000). Moreover, glaciers respond to changes in both temperature and precipitation, yet the methods used to reconstruct and interpret ELA changes

generally assume no change in precipitation. To improve ELA interpretations, it is useful to constrain either past temperature or precipitation. Unfortunately, there are very few records of tropical terrestrial temperatures, especially at high elevation, and most tropical precipitation records are qualitative. Thus, recently published moraine chronologies together with independent temperature reconstructions from alpine lakes in tropical East Africa (i.e., Kelly et al., 2014; Loomis et al., 2012, 2015, 2017) provide an excellent opportunity to compare and reconstruct past glacier extents, ELAs, and climate during and since the LGM.

Here, we present simulated glacier extents in the Rwenzori Mountains, located in Uganda and the Democratic Republic of Congo. We used a glacier model and independent temperature reconstructions from two high-elevation sites (2350 and 3081 m above sea level [asl)] on Mount Kenya to simulate a transient history of glacier change based on available paleoclimate data from East Africa. The independent temperature reconstructions are from changes in the relative abundances of branched glycerol dialkyl glycerol tetraether (brGDGTs) in lake sediments, which provide continuous temperature-change estimates over the past 31 k.y. (Loomis et al., 2012, 2017). We chose to model glaciers in the Rwenzori Mountains because this is one of the few locations in East Africa where moraines have been precisely dated, documenting glacier positions during the LGM (Kelly et al., 2014). Although moraine chronologies exist on Mount Kenya, they are based on ³⁶Cl ages, and the data, particularly for the LGM, show significant scatter (Shanahan and Zreda, 2000). Moreover, there are numerous undated moraines in the Rwenzori Mountains, and so we could use the simulations to estimate possible moraine ages.

We use the brGDGT-based temperature reconstructions to force six glacier model runs with various estimated temperature and precipitation changes, and we compared the transient simulated glacier extents with the moraine locations. One goal of this work was to assess whether the available paleoclimate data for East Africa can produce simulated glaciers that match the existing moraine chronology. Another goal was to examine the extents of Rwenzori glacier advances and retreats between times of moraine deposition. Moraine records are inherently discontinuous, and by using a glacier model, we can track changes in glacier extent, including ice-free conditions, in response to temperature forcing.

EAST AFRICAN PALEOCLIMATE

Kilimanjaro in Tanzania, Mount Kenya in Kenya, and the Rwenzori Mountains in Uganda and the Democratic Republic of Congo are the only currently glacierized locations in Africa (Fig. 1; Table S3¹). Equatorial East African alpine temperatures and lapse rates among these three locations are relatively similar to one another under modern conditions (Loomis et al., 2017), and we would expect to see similar magnitudes of temperature changes in alpine sites through time. We assumed that the general patterns of past precipitation change observed in the lowlands would apply to high-elevation sites as well.

Both temperature and precipitation are thought to have varied dramatically during the past ~31 k.y. in tropical East Africa. East African alpine temperature records are relatively rare and suggest larger temperature changes than at lower altitudes (Loomis et al., 2017). Loomis et al. (2012, 2017) reconstructed temperatures using brGDGTs from two remote alpine lakes on Mount Kenya (Fig. 1, inset): Sacred Lake (2350 m asl; Loomis et al., 2012) and Lake Rutundu (3081 m asl; Loomis et al., 2017). Together, these records cover the past ~31 k.y. and show generally similar trends in temperature through time (Fig. 2A), including LGM temperatures being 5.5-6.1 °C below modern temperatures, warming conditions by 15 ka (~2 °C below modern temperatures), a minor cooling ca. 13–11 ka, and a temperature maximum in the middle Holocene, at about ca. 6 ka. Aside from these general similarities, the records show differences in the timing and magnitude of cold events during the LGM and late glacial time. For example, the timing of maximum cooling in the Sacred Lake record occurs at ca. 24 ka (Fig. 2A, orange line), whereas the maximum cooling in the Lake Rutundu record occurs at ca. 18 ka (Fig. 2A, red line). In addition, the minor cooling at ca. 13–11 ka appears in both records, but the magnitude of cooling is greater in the Lake Rutundu record (4 °C below modern). Other East African paleoclimate proxy records also suggest temperature changes during late glacial time. For example, a TEX₈₆ temperature record (where TEX₈₆ indicates an index of tetraethers consisting of 86 carbon atoms in membrane lipids produced by mesophilic marine and lacustrine Thaumarchaeota) from Lake Tanganyika suggests a plateau in temperature during the Antarctic Cold Reversal, and colder temperatures at ca. 14.7 and 12.9 cal k.y. B.P. compared to temperature at 11.2 cal k.y.

B.P. (Tierney et al., 2008). Arid and cool conditions inferred from Lake Albert δD and TEX $_{86}$ records (Berke et al., 2014) occurred between 13.8 and 11.5 cal k.y. B.P.

Precipitation reconstructions from East Africa typically are from fossil pollen, lake-level changes, and water isotope records at relatively low-elevation sites. These records suggest that LGM conditions were between 10% and 30% drier than present-day values (Bonnefille et al., 1990; Shanahan et al., 2008), as exemplified by equatorial East African lake levels (i.e., Lakes Albert, Victoria, and Tanganyika), which were substantially lower than modern positions (e.g., Talbot and Livingstone, 1989; Beuning et al., 1997; Gasse, 2000). Postglacial precipitation estimates from δD plant waxes (Schefuß et al., 2005) and diatom assemblages (Haberyan and Hecky, 1987; Stager et al., 2011) suggest variable precipitation changes, with relatively wet conditions at 15-13 cal k.y. B.P. and during the "African Humid Period" (11– 5 ka), and dry conditions during Heinrich event 1 (17–16 ka) and the Younger Dryas (12.9-11.7 ka; Roberts et al., 1993; Gasse, 2000; Otto-Bliesner et al., 2014). Lake Albert (Fig. 1, inset) is ~100 km north of the modern Rwenzori glaciers, and sediment records from this lake show at least two mature paleosols that formed between ca. 21.7 and 14.8 cal k.y. B.P. (Beuning et al., 1997), both interpreted as relatively drier conditions. Dry conditions appear at ca. 11.4 cal k.y. B.P. in the palynological data (Beuning et al., 1997). The Lake Albert records also suggest a shift toward wetter conditions at ca. 14.8 cal k.y. B.P., subsequent to the LGM aridity. Lake Edward (Fig. 1, inset) is ~50 km south of the modern Rwenzori glaciers, and sediment records from this lake indicate a wet early Holocene, the onset of drier conditions at 5.2 cal k.y. B.P., which culminated in a late Holocene lowstand between 4 and 2 cal k.y. B.P., and a rapid lake-level rise to modern positions by ca. 1.7 cal k.y. B.P. (Russell et al., 2003).

RWENZORI MOUNTAINS

The Rwenzori Mountains (0°23'N, 29°53'E; Fig. 1) are an uplifted horst block in the western arm of the East African Rift, and they contain three glacierized areas on Mount Baker, Mount Speke, and Mount Stanley (with a peak elevation of 5109 m asl). Snowline altitude estimates from CE 1955 range from 4500 to 4720 m asl, with an average of 4600 m asl, excluding Moore Glacier on Mount Baker (Osmaston, 1989). The modern Rwenzori glaciers terminate above 4750 m asl on Mount Stanley (Lentini et al., 2011), are out of equilibrium with the climate, and are predicted to melt away completely in the near future (Taylor et al., 2006). The total annual precipitation varies spatially across the mountain range, with the highest values (up to 2.6 m yr⁻¹; Osmaston, 1989) in the southeast portion of the range (Fig. S1 [see footnote 1]). Mountain glaciers that receive ample precipitation, such as those in the Rwenzori Mountains, are more sensitive to changes in temperature than glaciers in drier settings (Kaser, 2001; Oerlemans, 2001). This difference is due to a stronger albedo feedback on high-precipitation glaciers, the temperaturedependent partitioning between rain and snow, and an increase in

^{&#}x27;Supplemental Material. Explanation of the modeling methods, climate input data, and a comparison between glacierized sites in East Africa. Please visit https://doi.org/10.1130/SPE.S.12990986 to access the supplemental material, and contact editing@geosociety.org with any questions.

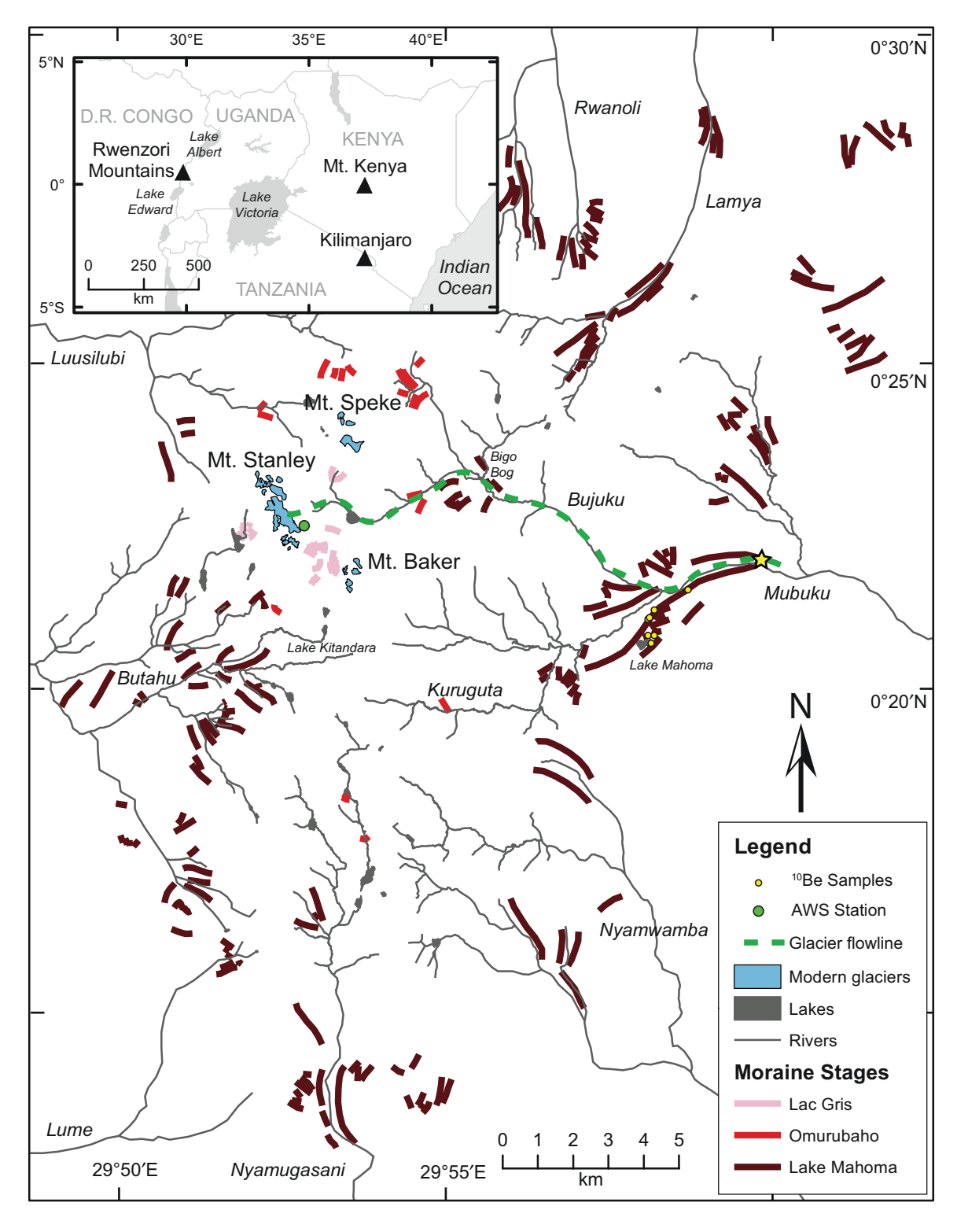


Figure 1. Map showing the central Rwenzori glaciers and moraines (mapped moraines based on Kaser and Osmaston, 2002; Osmaston, 2004) with an inset map showing the proximity of the Rwenzori Mountains to Mount Kenya and Kilimanjaro. Green dashed line marks the central flowline from which we calculated glacier lengths. ¹⁰Be age samples (yellow dots) of Lake Mahoma stage moraines in the Mubuku valley indicate moraine deposition at 24.9 and 21.5 ka, during the Last Glacial Maximum (LGM; Kelly et al., 2014). An automatic weather station (AWS; green dot) is located at 4750 m above sea level (asl) and provided climate data used in the glacier model (Lentini et al., 2011). A yellow star marks the location of the LGM target. D.R. Congo—Democratic Republic of Congo.

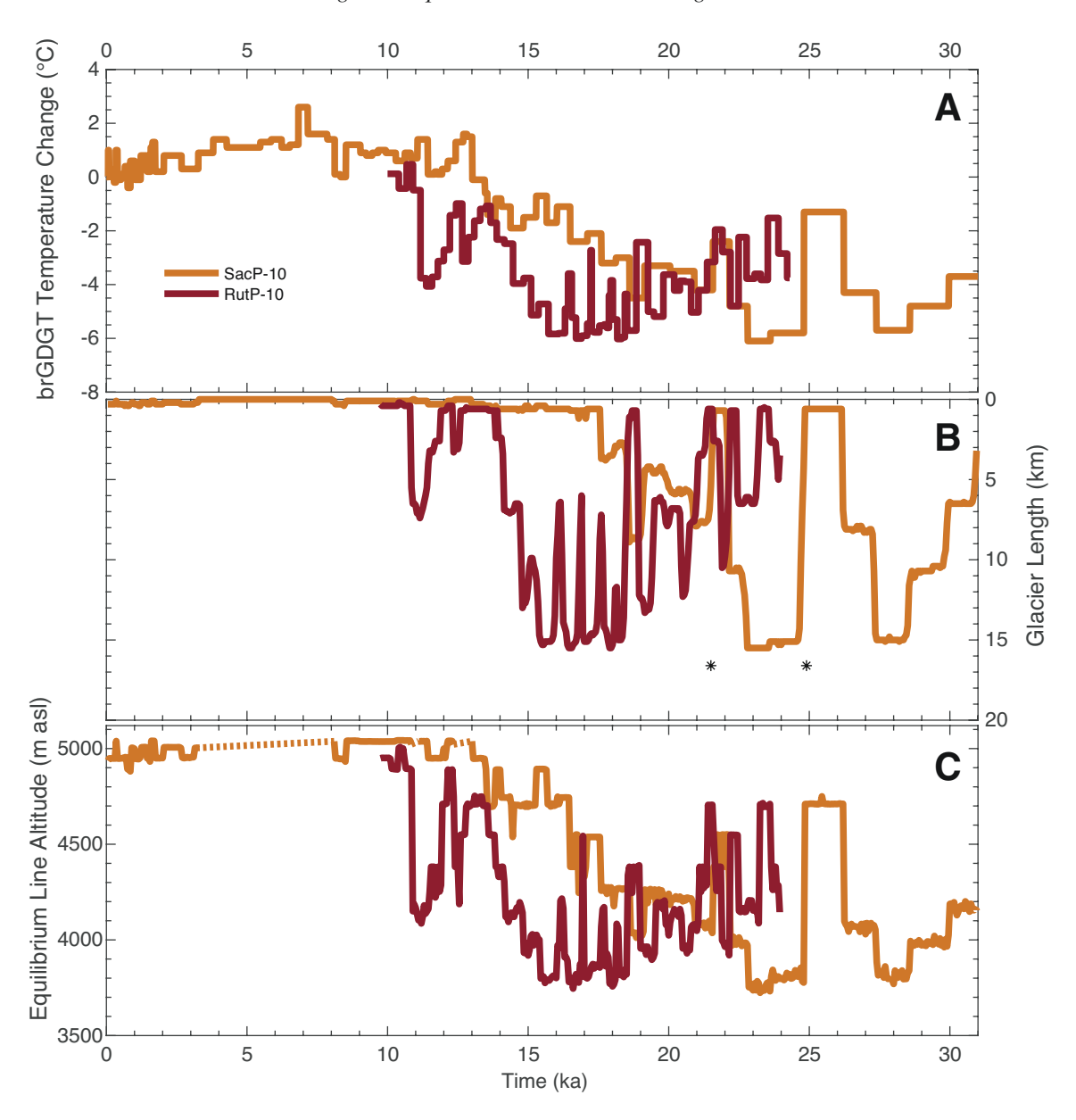


Figure 2. Plots showing input temperatures, simulated glacier lengths, and equilibrium line altitudes (ELAs) for simulations SacP-10 and RutP-10. (A) Input temperature sequences based on the branched glycerol dialkyl glycerol tetraether (brGDGT) temperature reconstructions from Sacred Lake (SacP-10, orange line) and Lake Rutundu (RutP-10, red line) using a nearest-neighbor interpolation between data points. (B) Simulated glacier length in the Mubuku and Bujuku valleys over time when forced by the different temperature reconstructions and precipitation estimates. Black asterisks represent the ages and glacier lengths of the Last Glacial Maximum (LGM) moraines in Mubuku valley (Kelly et al., 2014). (C) Fluctuations in the modeled ELA from 31 to 0 ka relative to the ELA estimates for the Lake Mahoma, Omurubaho, and Lac Gris stages (dashed lines indicate ice-free conditions; asl—above sea level).

ablation because high-precipitation glaciers extend further down valley (Oerlemans, 2001, p. 51).

Valleys that radiate from the central Rwenzori peaks contain moraines that mark past glacier extents (Fig. 1). Osmaston (1989) and Kaser and Osmaston (2002) grouped these moraines into five stages based on weathered appearance, boulder abundance, and proximity to the modern glaciers. Here, we focused on the three

most recent stages: the Lake Mahoma stage, the Omurubaho stage, and the Lac Gris stage, and we compared the model results herein with the detailed map from Kaser and Osmaston (2002).

Lake Mahoma stage moraines can be more than 50 m in relief and reach elevations as low as 2070 m asl, ~16 km down valley from the modern glaciers. Lake Mahoma stage moraines have been dated to ca. 24.9 ± 0.5 and 21.5 ± 0.7 ka (i.e., during

the LGM) in the Mubuku valley (Fig. 1; Kelly et al., 2014). Osmaston (1989) reconstructed ELAs for the Lake Mahoma stage glacier extents using the graphical height and the areaheight-accumulation methods. These reconstructed ELAs varied across the mountain range from ~3600 m asl in the east to ~4100 m asl in the west (Table S1 [see footnote 1]; Osmaston, 1989, 2004; Kaser and Osmaston, 2002). Osmaston (1989) attributed the east-west ELA gradient to the precipitation gradient (Fig. S1), with wetter conditions in the southeast Rwenzori Mountains compared to the northwest portion of the range. Osmaston (1989) estimated the ELA of the LGM-dated ice extent in the Mubuku valley to be ~3600 m asl, which is a ΔELA of ~1000 m (i.e., the ΔELA is the difference between the ELA at a specified time in the past and the average CE 1955 ELA of 4600 m asl), or 880 m if accounting for the 120 m decrease in global sea level during the LGM (Osmaston, 1989). All further discussions of $\Delta ELAs$ in this manuscript do not account for the 120 m decrease in global sea level. Based on the Lake Mahoma stage ELA estimates of 4100-3600 m asl (west to east region, respectively), Osmaston (1989) estimated ΔELA values of 500–1000 m, with smaller $\Delta ELAs$ in the western portion of the Rwenzori Mountains. This ΔELA range is similar to that (503– 1387 m) reported by Mark et al. (2005) for the Lake Mahoma stage (Osmaston, 1989; Kaser and Osmaston, 2002). Porter (2000), however, identified the Rwenzori as an outlier among tropical glacier records because he estimated a Lake Mahoma stage ΔELA of 620–670 m in the Rwenzori Mountains, which is ~70% of the tropical average LGM Δ ELA of 925 \pm 115 m.

Omurubaho stage moraines are $\sim 10-20$ m in relief and occur between 3600 and 4000 m asl, $\sim 3-7$ km down valley from the modern glaciers (Kaser and Osmaston, 2002). The Omurubaho stage moraines have poor age control. A single minimum-limiting radiocarbon age of 7.7 cal k.y. B.P. for this stage from Lake Kitandara (4000 m asl; Fig. 1) places the moraines in the early Holocene Epoch or possibly late glacial time (Livingstone, 1967). The Omurubaho stage ELA estimates in the Bujuku valley are ~ 4390 m asl, which is a Δ ELA of ~ 210 m (Osmaston, 1989).

Lac Gris stage moraines are ~5–10 m in relief and occur above 4000 m asl, within 1–2 km of the modern glaciers. Lac Gris stage moraine ages based on the growth of *Senecio friesio*-

rum and soil development are ca. 0.7–0.1 cal k.y. B.P. (de Heinzelin, 1953; Osmaston, 1989). The Lac Gris stage ELA estimates in the Bujuku valley are ~4520 m asl, which is a Δ ELA of ~80 m (Osmaston, 1989).

METHODS

Glacier Model Setup and Validation

We used a glacier model and East African temperature reconstructions to simulate transient glacier changes in the Rwenzori Mountains from 31 ka to present. The glacier model is a coupled two-dimensional (2-D) ice-flow and mass-balance model, which includes a spatially distributed energy-balance model (Oerlemans, 1992; Anderson et al., 2010; Doughty et al., 2013). The 2-D (vertically integrated) ice-flow component is based on the shallow ice approximation and includes basal sliding (Kessler et al., 2006) and internal deformation equations (Plummer and Phillips, 2003). The mass-balance model partitions precipitation into rain and snow based on the temperature at each grid cell and a snow-rain temperature threshold of 2.5 °C (Mölg et al., 2008). The mass-balance output is based on an energy-balance model of intermediate complexity (Anderson et al., 2010), and it accounts for complex terrain features, such as shading, aspect, slope, and elevation. We included day-to-day temperature variability with a mean equal to the monthly temperature value (Table 1). The iceflow model computes glacier flow on a yearly basis and outputs an updated ice thickness for the mass-balance model. The iceflow model calls the mass-balance model once every 10 model years, which is ideal for transient simulations because the glacier configuration is updated as the input climate changes. The glacier model produces ice thickness and mass-balance values for the entire model domain (central Rwenzori, Fig. 1) and saves these values every 50 model years in each simulation.

The model has successfully produced modern and past glacier extents in New Zealand (Anderson et al., 2010; Doughty et al., 2013, 2017), and here we applied it to glaciers in the Rwenzori Mountains. We did not alter the model itself, but the input values, including mountain topography, modern spatially distributed monthly mean climate, and changes from modern climate,

TABLE 1. MODERN CLIMATE INPUT DATA AND SOURCES

Variable	Values	Source
Temperature	-0.35 °C at 4750 m above sea level	Lentini et al. (2011)
Modern temperature lapse rate	0.0058 °C m ⁻¹	Loomis et al. (2017)
Day-to-day temperature variability	1 °C	0.8 °C in Lentini et al. (2011)
Annual precipitation total	Spatially variable	Osmaston (1989)
Monthly precipitation proportions	Supplemental material	New et al. (2002)
Relative humidity	90.4%	Lentini et al. (2011)
Wind speed	3.58 m s^{-1}	Lentini et al. (2011)
Incoming solar radiation	Supplemental material	Lentini et al. (2011)
Note: See text footnote 1 for supplemen	ital material.	

are all specific to the Rwenzori Mountains. We tested and validated the model by simulating modern glacier extents (CE 1955; Kaser and Osmaston, 2002) on the three currently glacierized peaks in the range at 100 m resolution (supplementary material, Fig. S2 [see footnote 1]).

Using a glacier model to reconstruct past ELAs is different from other methods, such as the accumulation area ratio method or toe-headwall altitude ratio method, in two important ways. First, the model can be used to evaluate the impact a change in temperature, precipitation, or other environmental variables has on glacier mass balance, thickness, and length. Second, the model applies the changes in temperature and precipitation to the entire mountain range and allows the physics of glacier flow and mass balance determine glacier extent. Therefore, using the brGDGT temperature reconstructions as model input, we can simulate glacier maxima through time and estimate possible ages of moraines near those glacier maxima.

Model Input

We used a 100-m-resolution digital elevation model (DEM; SRTM_v4; Jarvis et al., 2008) to represent the land surface. We did not remove the modern ice thickness from the land surface because the ice thickness has not been measured, and the present-day glacier area is relatively small (<1 km²; Taylor et al., 2006; Worldview 1 imagery, 2006). We did not account for changes in the shape or elevation of the mountain range, which has an average uplift rate of 0.5 mm yr⁻¹ (Kaufmann and Romanov, 2012). This uplift should not influence our results.

The existing modern climate data from the Rwenzori Mountains are sufficient to run the glacier model; however, the short duration of climate data collection introduces some uncertainty in the simulations. Modern climate input data for the model are from a range of sources (Table 1; Table S2 [see footnote 1]). Monthly mean temperatures are from an automatic weather station located on Mount Stanley at 4750 m asl (Fig. 1, green dot), which ran from CE 2006 to 2009 (Table S2; Lentini et al., 2011). Temperatures decrease with elevation according to the modern observed lapse rate of 5.8 °C km⁻¹ (Loomis et al., 2017). Although the lapse rate was steeper during the LGM (Loomis et al., 2017), we chose to use the modern lapse rate in the simulations because the brGDGT-based temperature records from Mount Kenya are from relatively high elevations (2350 and 3081 m asl), close to the elevations of the LGM glacier ablation area.

Annual precipitation data were based on measurements taken from CE 1951–1954 (Osmaston, 1989). The data vary spatially and reveal a gradient from wetter conditions in the southeastern Rwenzori to drier conditions in the western portion of the range (Fig. S1; Osmaston, 1989). We partitioned the annual rainfall into monthly values following Climatic Research Unit estimates for the Rwenzori area (New et al., 2002). The two rainy seasons in March to May and September to November are reflected in the monthly values (Table S2). The Rwenzori Mountains are notorious for significant cloud

cover, high humidity, and rainfall up to 2.6 m of precipitation annually (Osmaston, 1989).

Transient Simulations

We ran six transient glacier simulations using temperature reconstructions from Mount Kenya and estimates of precipitation based on prior work. Thus, for all simulations, the input temperature change varied through time, whereas input precipitation change was held constant through time.

The input temperature change from modern values (ΔT) was from two brGDGT-based temperature reconstructions from lakes on Mount Kenya (Fig. 2A; Loomis et al., 2012, 2017). The record from Sacred Lake (0°05'N, 37°32'E, 2350 m asl; Loomis et al., 2012) spans the time period of 31-0 ka, has a temperature uncertainty of ± 0.8 °C, and has an age uncertainty of 0.5 k.y. (Loomis et al., 2012, 2015). The age model for this record was based on 29 radiocarbon dates calibrated to calendar years using Calib 6.0 and interpolated using mixed-effect regression (Loomis et al., 2012). The record from Lake Rutundu (0°03'N, 37°28'E, 3081 m asl; Loomis et al., 2017) spans the time period 24.3–0 ka, has a temperature uncertainty of ±0.6 °C, and has an age uncertainty of 0.6 k.y. (Loomis et al., 2017). The age model for this record was based on 10 210 Pb ages and 19 radiocarbon ages calibrated to calendar years using Intcal13 (Loomis et al., 2017). For simplicity, we refer to ages from these records as "ka" and refer to age intervals from these records as "k.y." We connected data points in these temperature records using a nearest-neighbor interpolation, which creates abrupt, step changes in ΔT values relative to smooth or gradual changes in temperature between sample points. One benefit of including step changes is to see how quickly the simulated glacier responds to these abrupt temperature changes. Input precipitation change from modern values (ΔP) was based upon estimates of LGM precipitation from East African lakes (Gasse, 2000, and references therein). Most precipitation records are qualitative, and the majority of the records suggest that the LGM was drier than modern conditions in equatorial East Africa. Specifically, quantitative estimates suggest ΔP values of -10% to -30% (Shanahan et al., 2008) for equatorial East Africa.

To reduce the influences of the temperature uncertainties, high sample-to-sample variability, and differences between the two temperature records on model simulations, we calculated the average of the two temperature reconstructions (Fig. 3, gray line). We also calculated a 500 yr running mean of the averaged temperature records to smooth sample-to-sample variability (Fig. 3, black line). The "MeanP-10" simulation used an average of the interpolated Sacred Lake and Lake Rutundu temperature reconstructions during the period 23.5–0 ka. The "500yrP-10" simulation used a 500 yr running mean of the average interpolated Sacred Lake and Lake Rutundu temperature records for the time period 23.5–0 ka (Table 2). These simulations both used a ΔP of -10%, which is a conservative estimate, and by simulating drier LGM conditions (ΔP of -20% to -30%), the model would produce shorter glaciers under the same temperature regime.

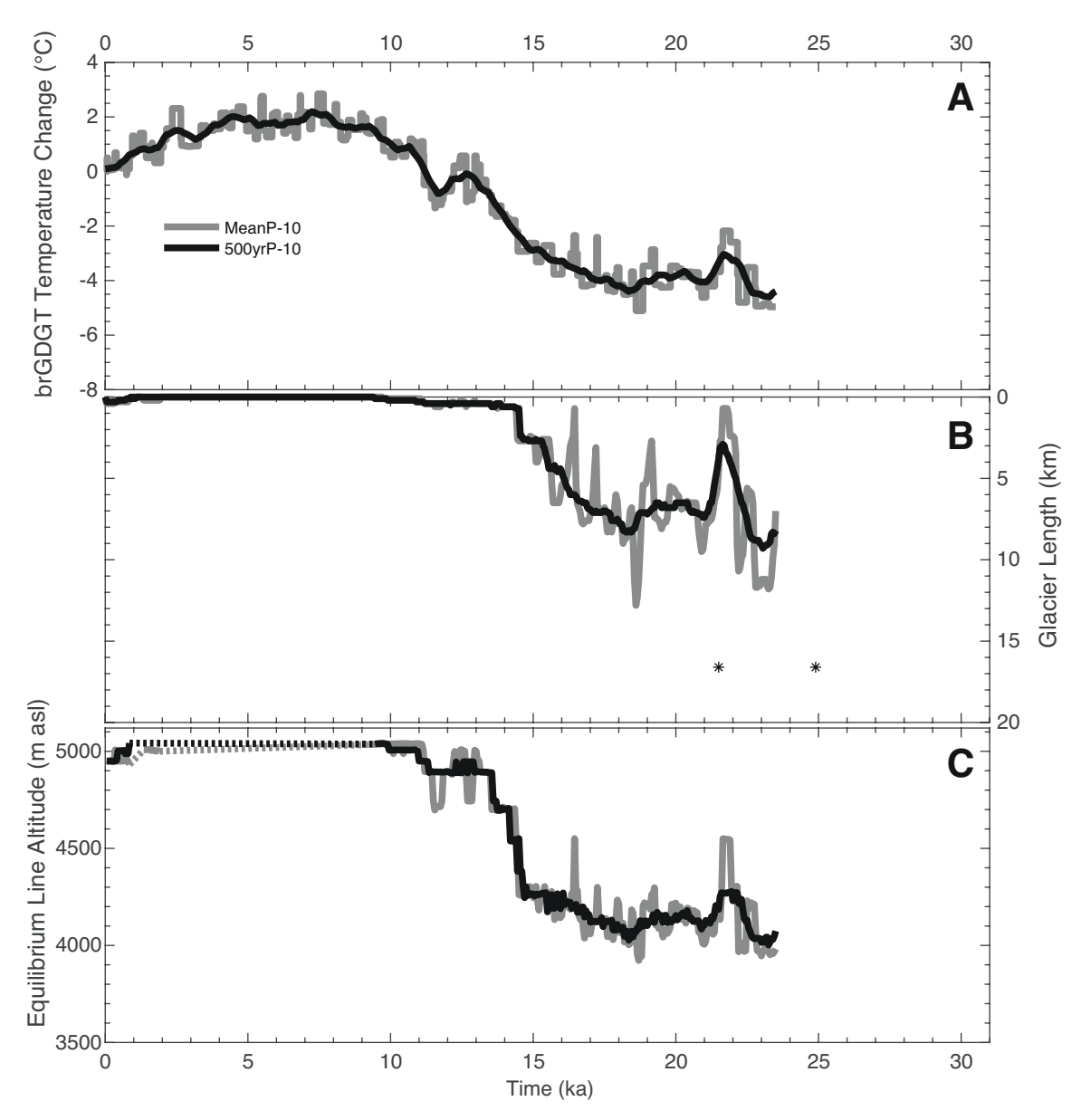


Figure 3. Plots showing (A) input temperature, (B) simulated glacier lengths, and (C) calculated equilibrium line altitudes (ELAs) for simulations MeanP-10 (gray line) and 500yrP-10 (black line). Black asterisks represent the ages and glacier lengths associated with the Last Glacial Maximum (LGM) target (Kelly et al., 2014). Dashed lines indicate ice-free conditions where the ELA is above the simulated mountain peak; brGDGT—branched glycerol dialkyl glycerol tetraether; asl—above sea level.

TABLE 2. MODEL SIMULATION TEMPERATURE CHANGE AND PRECIPITATION CHANGE

INPUT FROM MODERN CLIMATE								
Simulation	Temperature record	Precipitation	Period					
MeanP-10	Averaged	-10%	23.5-0 ka					
500yrP-10	500 yr running mean	-10%	23.5-0 ka					
SacP-10	Sacred Lake	-10%	31-0 ka					
RutP-10	Lake Rutundu	-10%	24.3-10 ka					
MeanP+30	Averaged	+30%	23.5-16 ka					
500yrP+30	500 yr running mean	+30%	23.5-16 ka					

The second two simulations, "SacP-10" and "RutP-10," used the Sacred Lake temperature record (Loomis et al., 2012) and the Lake Rutundu temperature record (Loomis et al., 2017), respectively, without smoothing to explore whether millennial-scale temperature variability would produce glacier extents close to the moraine positions. Both simulations used a ΔP of -10%. SacP-10 covered the period 31–0 ka (Fig. 2A, orange line), whereas RutP-10 covered the period 24.3–10 ka (Fig. 2A, red line; Table 2).

The final two simulations, "MeanP+30" and "500yrP+30," tested the sensitivity of the Rwenzori glaciers at their maximum extents to changes in precipitation, with both simulations using

a ΔP of +30%. MeanP+30 focused on the time period 23.5–16 ka and used the average of the Sacred Lake and Lake Rutundu records (Fig. 4A, light blue line). Simulation 500yrP+30 used a 500 yr running mean of the average of the interpolated Sacred Lake and Lake Rutundu temperature records for the period 23.5–16 ka (Fig. 4A, dark blue line; Table 2). We are not suggesting that precipitation increased during the LGM, but we were interested in these simulations as a way to evaluate the precipitation sensitivity of these glaciers. We compared the glacier extents in MeanP-10 with MeanP+30 and 500yrP-10 with 500yrP+30 for the period 23.5–16 ka.

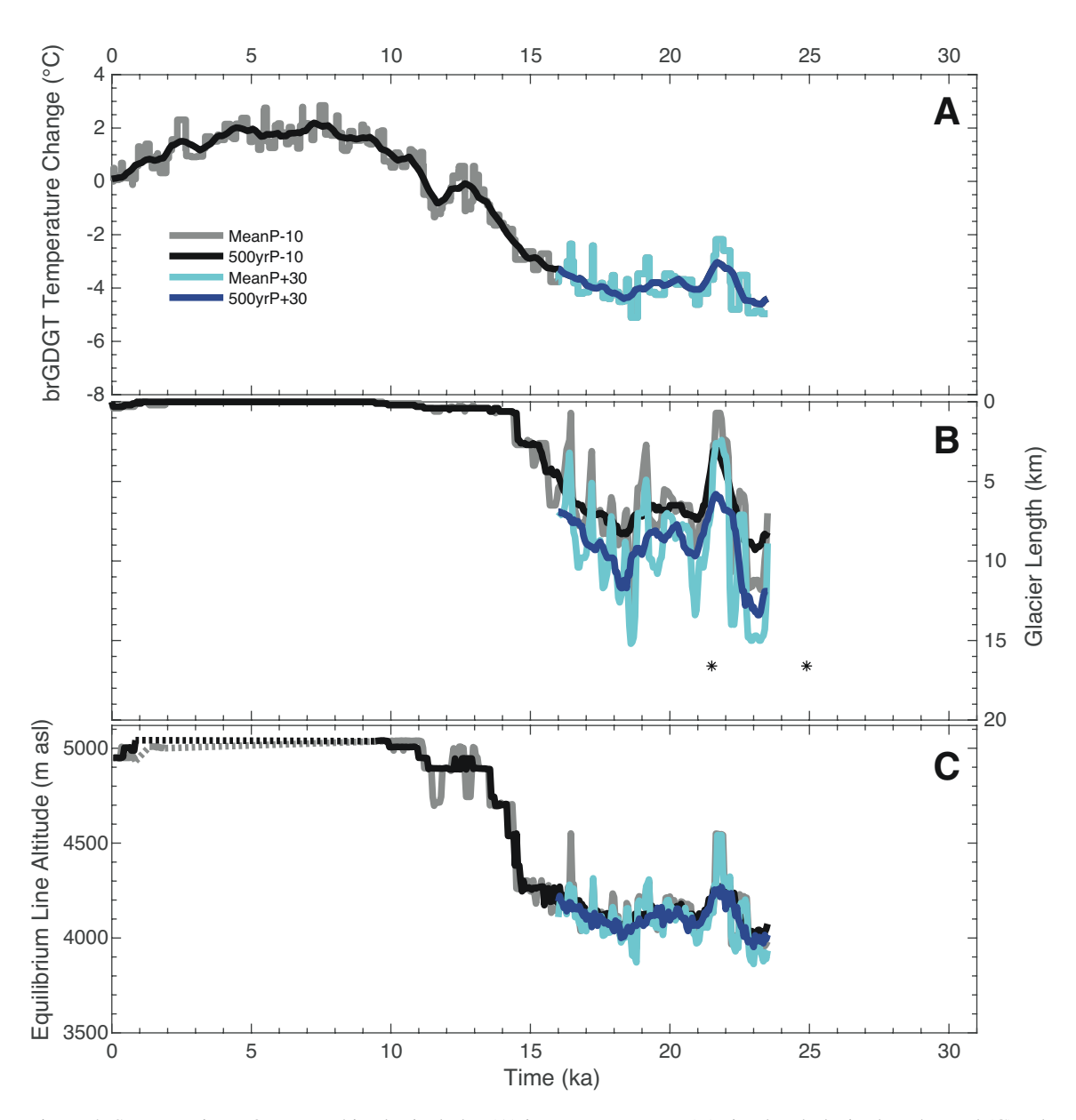


Figure 4. Same as Figure 3, except this plot includes (A) input temperature, (B) simulated glacier lengths, and (C) calculated equilibrium line altitudes (ELAs) for simulations MeanP+30 (light blue line) and 500yrP+30 (dark blue line) as well; brGDGT—branched glycerol dialkyl glycerol tetraether; asl—above sea level.

We calculated glacier length changes in the Bujuku and Mubuku valleys (Fig. 1, center flowline along the green dashed line) over time from the ice thickness output and compared these lengths with the moraines in the Bujuku and Mubuku valleys. This flowline begins at the highest glacierized area (Mount Stanley), which is likely to be the last location for glaciers to melt away and the first to initiate glacier growth. When the simulated glacier length is 0 km in the Bujuku valley, ice-free conditions persist throughout the model domain.

We compared the simulated glacier lengths to an inferred LGM terminal moraine, referred to here as the "LGM target" (Fig. 1, yellow star), which is geomorphically connected to the dated LGM moraines in the Mubuku valley (Kelly et al., 2014; Fig. 1, yellow dots). The Lake Mahoma stage moraines relate to glacier lengths between 7 and 16.6 km, where 16.6 km matches the LGM target position. The shorter lengths (i.e., ~7 km) relate to moraines in the Bigo Bog area (Fig. 1), which were interpreted as Lake Mahoma stage in Kaser and Osmaston (2002) and as Omurubaho stage in Osmaston (1989). Because we followed Kaser and Osmaston (2002), we treated the Bigo Bog moraines as Lake Mahoma stage. The Omurubaho stage moraines relate to glacier lengths between 4.5 and 7 km. Last, the Lac Gris stage moraines relate to glacier lengths between 0.7 and 1.4 km.

We calculated ELAs by averaging the elevations (DEM and modeled ice thickness) in the grid cells on the glacier in the Bujuku and Mubuku valleys that had an annual mass balance >-0.2 and <0.2 m yr⁻¹. Finally, we compared changes in modeled ELAs with previous ELA estimates for the Rwenzori Mountains and the tropics (Osmaston, 1989; Porter, 2000; Mark et al., 2005).

RESULTS

We successfully simulated the CE 1955 glacier extents on the three currently glacierized peaks in the Rwenzori Mountains at 100 m resolution (Fig. S2). In order to model these glacier extents, we used a ΔT of -1 °C and a ΔP of 0% and modern values for the other input climate parameters (Table 1).

All simulations formed glaciers during the LGM that terminated between Bigo Bog in the Bujuku valley and the outermost Lake Mahoma stage moraines in the Mubuku valley. One of the simulations suggested a glacier readvance during the late glacial to early Holocene. The simulations suggested the possibility of rapid glacier advance and retreat caused by the fluctuations in the brGDGT temperature records (Figs. 2A and 2B; Fig. S3).

Here, we describe the timing of the simulated glacier advances and whether the simulated glacier extents reached the Lake Mahoma, Omurubaho, and Lac Gris stage moraines. We estimated moraine ages based on when the simulated glacier extent was 90%–110% of the length needed to reach the most down-valley moraine of interest. Glacier lengths that were within these bounds for the LGM target, for example, ranged from 14.9 to 18.3 km. All glacier lengths reported here (Figs. 2B, 3B, and 4B) were from the simulated glacier that occupied the Bujuku valley (Fig. 1, green dashed line), referred to as the Bujuku valley glacier.

Simulated Glacier Lengths during the LGM

Output from the MeanP-10 simulation showed the Bujuku valley glacier lengths as 11.9 km (72% of the length needed to reach the LGM target) at 23.3 ka, and 12.8 km (77% of the length needed to reach the LGM target) at 18.6 ka (Fig. 3B, gray line; Table 3). The 500yrP-10 simulation output showed the maximum Bujuku valley glacier lengths as 9.3 km (56% of the length needed to reach the LGM target) at 23 ka (Fig. 5B), and 8.3 km (50% of the length needed to reach the LGM target) at 18.4 ka (Fig. 3B, black line; Table 3). The averaged temperature curves used in these simulations had a magnitude of cooling (i.e., -5.1 °C to -4.4 °C) large enough to force the simulated glacier to between 77% and 50% of the length needed to reach the dated

TABLE 3. CLIMATE CONDITIONS AND INFERRED TIMING FOR THE MOST EXTENSIVE GLACIER EXTENTS IN EACH SIMULATION

Simulation	ΔP (%)	ΔT(°C)	Date (ka)	Length (km)	Length relative to LGM (%)	ELA (m above sea level)	ΔELA (m)
MeanP-10	-10	-5.0	23.3	11.9	72	3950	650
	-10	-5.1	18.6	12.8	77	3920	680
500yrP-10	-10	-4.6	23.0	9.3	56	4020	580
	-10	-4.4	18.4	8.3	50	4030	570
SacP-10	-10	-6.1	22.8	15.5	93	3720	880
RutP-10	-10	-6.0	18, 16.5	15.5	93	3750	850
MeanP+30	+30	-5.0	23.3	15.0	90	3880	720
	+30	-5.1	18.6	15.2	92	3910	690
500yrP+30	+30	-4.6	23.0	13.2	80	3950	650
	+30	-4.4	18.4	11.7	70	4010	590

Note: Simulated glacier length relative to the length needed to reach the dated Last Glacial Maximum (LGM) moraine in the Mubuku valley is reported as a percentage. ΔP —change in precipitation; ΔT —change in temperature; ELA—equilibrium line altitude; ΔELA —change in equilibrium line altitude.

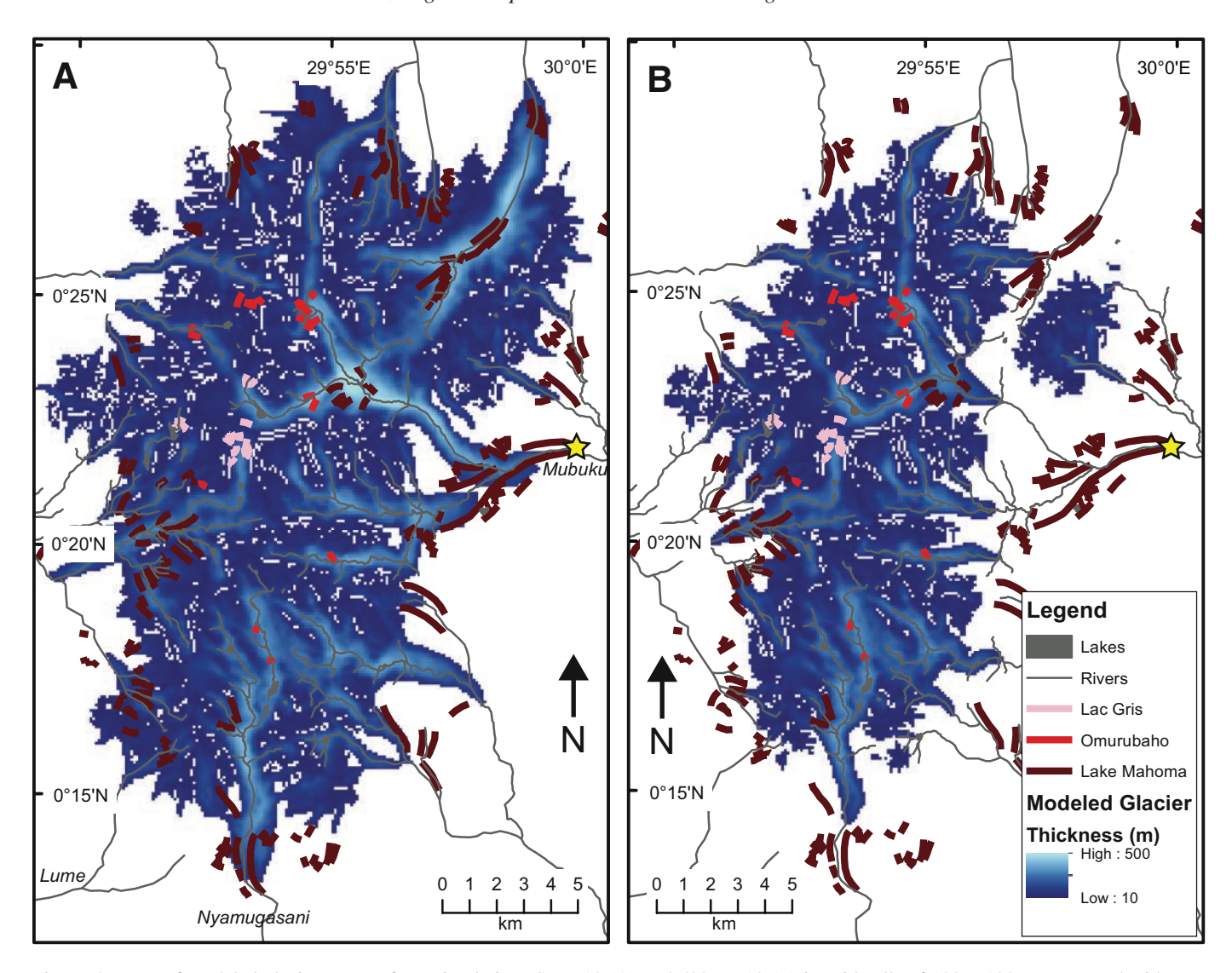


Figure 5. Maps of modeled glacier extents from simulations SacP-10 (A) and 500yrP-10 (B) in grid cells of 100×100 m compared with moraines. Panel A shows modeled ice thickness at 22.8 ka, with a change in temperature (ΔT) of -6.1 °C and a change in precipitation (ΔP) of -10% from modern conditions. Panel B shows modeled ice thickness at 18.4 ka with a ΔT of -4.4 °C and a ΔP of -10%. Yellow star in panel A marks the position of the Last Glacial Maximum (LGM) target in Mubuku valley.

LGM target. Neither of these simulations resulted in the glacier reaching the moraine.

Output from the SacP-10 simulation showed the maximum Bujuku valley glacier length as 15.5 km (93% of the length needed to reach the LGM target) at 23.6–22.8 ka (Fig. 5A; Fig. 2B, orange line; Table 3). The RutP-10 simulation produced a maximum Bujuku valley glacier length of 15.5 km at 18 and 16.5 ka (Fig. 2B, red line; Table 3). Both of these simulations showed rapid glacier fluctuations caused by the step changes produced by the interpolation scheme and the sample-to-sample variability in the temperature records. These rapid glacier length changes showed the Bujuku valley glacier advancing close to the LGM moraines and then retreating to modern glacier extents several times within the LGM.

Simulated Glacier Lengths during the Late Glacial

The different records simulated different initial timings and rates of retreat from the LGM positions. Retreat was earliest in the SacP-10 simulation and began later in the MeanP-10, 500yrP-10, and RutP-10 simulations. In all simulations, the glaciers reached lengths of <1 km by 15 ka (Figs. 2B, 3B, and 6B). For example, the longest simulated glacier extent between 15 and 11 ka in MeanP-10 was ~0.6 km and occurred at 11.6 ka due to a ΔT of -1.3 °C and a ΔP of -10% (Fig. 6B). The Lake Rutundu record, however, includes two late glacial/early Holocene cooling events that produce glacier advances. The RutP-10 simulation output showed a minor advance of the Bujuku valley glacier (reaching a length of 3.3 km) at 12.4 ka, associated with

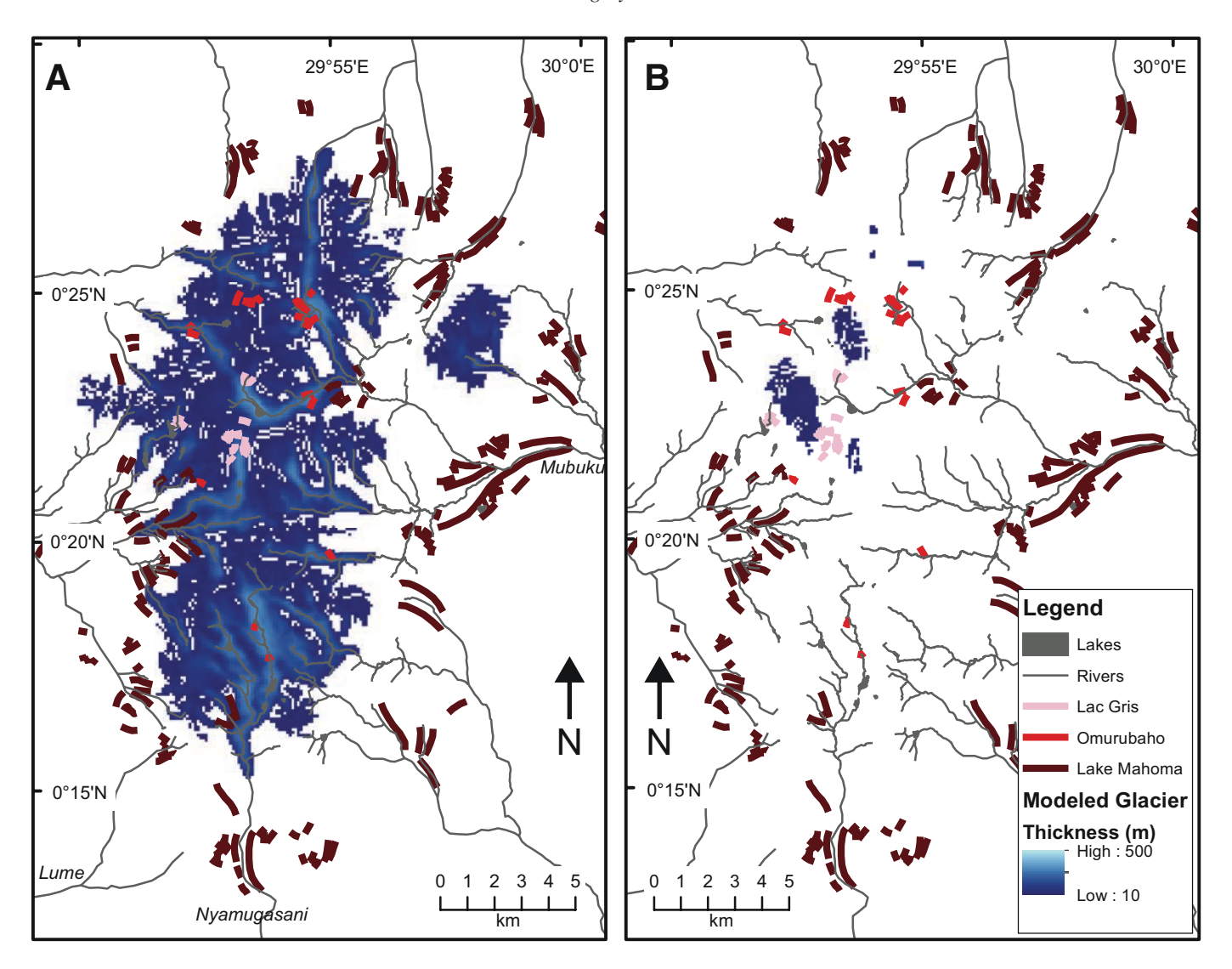


Figure 6. Maps of modeled glacier extents from simulation RutP-10 (A) and MeanP-10 (B) in grid cells of 100×100 m compared with moraines. Panel A shows modeled ice thickness at 11.2 ka, with a change in temperature (ΔT) of -4 °C and a change in precipitation (ΔP) of -10% from modern conditions. Panel B shows modeled ice thickness at 11.6 ka with a ΔT of -1.3 °C and a ΔP of -10%.

a ΔT of -3.1 °C. This Bujuku valley glacier length is too short to reach the mapped Omurubaho Stage moraines, which occur ~1.2 km farther down valley (Fig. 2B, red line). In the same simulation, another advance of the Bujuku valley glacier (reaching a length of 7.4 km) occurred at 11.2 ka and was associated with a ΔT of -4 °C. In this case, the Bujuku valley glacier length reached some mapped Lake Mahoma stage moraines near Bigo Bog (Figs. 1 and 6A).

Simulated Glacier Lengths during the Holocene

Three of the simulations included the entire Holocene Epoch (i.e., SacP-10, MeanP-10, and 500yrP-10). We did not extend the simulations through the Holocene using the Lake Rutundu

record because the Lake Rutundu and Sacred Lake records are very similar during this time. All three Holocene simulations used a ΔP of -10% carried over from the paleoclimate estimates for the LGM. Therefore, these simulations did not allow for times of increased precipitation relative to modern that occurred during the early Holocene African Humid Period in northern and equatorial Africa (Gasse, 2000).

All of the simulations that covered the Holocene showed Bujuku valley glacier lengths of <0.4 km, which is less than the Bujuku valley glacier lengths needed to reach the mapped Lac Gris stage moraines (0.7–1.4 km). The MeanP-10 simulation output showed ice-free conditions from 9.7 to 1.9 ka, and the Bujuku valley glacier at a Holocene maximum extent of 0.4 km between 0.3 and 0.1 ka (Fig. 3B, gray line). The 500yrP-10

simulation output showed ice-free conditions from 9.4 to 1 ka in the Rwenzori Mountains, and the Bujuku valley glacier at a Holocene maximum extent of 0.3 km at ~0.4-0 ka (Fig. 3B, black line). The Sacred Lake and Lake Rutundu records indicate maximum ΔT values of +2.2 to +2.8 °C during the middle Holocene. The simulated glaciers existed with ΔT values <+0.8 °C, but ΔT greater than +0.9 °C (with a ΔP of -10%) could cause ice-free conditions. The SacP-10 simulation output showed the Bujuku valley glacier length as 0.4 km at ca. 8.4 ka, followed by ice-free conditions in the Rwenzori Mountains from 8.0 to 3.3 ka due to ΔT of +0.9 °C (Fig. 2C, dashed lines). A slight decrease in temperature (ΔT of +0.3 °C) at 3.2 ka allowed glaciers to form again, and the Bujuku valley glacier reached a late Holocene maximum length of ~0.4 km at ca. 1.2, 0.8, and 0.7 ka. We recognize that the slightly lower elevation of the simulated mountain peak (i.e., 5020 m asl as opposed to the actual elevation of 5109 m asl) and the ΔP of -10% cause glaciers to melt sooner than they would under modern conditions. The Holocene ΔT values of +2.2 to +2.8 °C in the Sacred Lake and Lake Rutundu records would generate ice-free conditions even with a 5109 m asl elevation and a ΔP of 0%.

Simulated Glacier ELAs

The Δ ELAs were ~680–570 m in the MeanP-10 and 500yrP-10 simulations, respectively, during the LGM (Fig. 3C). The glacier length associated with a Δ ELA of 680 m is 77% of the length needed to reach the LGM target, and, therefore, the Δ ELA must have been >680 m for the glacier to advance to the LGM moraine. ELAs rose rapidly to near the CE 1955 level by 13 ka. From 9 to 2 ka, ELAs were above 5000 m asl (Fig. 3C, dashed lines).

The SacP-10 and RutP-10 simulations produced more ELA variability, with Δ ELAs of ~880–850 m during the LGM (Fig. 2C). Because these simulations did not reach the LGM moraines, the Δ ELA must have been larger than 880 m during the LGM. The late glacial to early Holocene glacier extent simulated in RutP-10 is associated with a Δ ELA of 510 m (Fig. 2C, red line). Simulated ELAs during the middle Holocene exceeded the maximum elevation of the mountains in the model (5020 m asl). The SacP-10 simulation produced the lowest Holocene ELA (4880 m asl), 280 m above the CE 1955 ELA, at 0.9 ka (Fig. 2C, orange line).

Glacier Length Sensitivity to Temperature and Precipitation

We estimated glacier length sensitivity to temperature and precipitation changes (independently) by comparing model input parameter values (i.e., temperature or precipitation change) and glacier lengths between simulations that shared all the same input except for one parameter (Table 3). Glacier length sensitivity depends on a number of factors, including climate and glacier hypsometry, and thus, these sensitivity values vary with glacier length. The difference in maximum Bujuku

valley glacier length during the LGM between the SacP-10 and 500yrP-10 simulations was 6.2 km due to a difference in ΔT of 1.5 °C (Fig. 5; Table 3). These values suggest a glacier length sensitivity to temperature during the LGM of ~4 km per 1 °C temperature change. The difference in maximum glacier length between MeanP-10 and MeanP+30 was 2.4 km due to a difference in ΔP of 40% (Table 3). These values suggest a glacier length sensitivity to precipitation during the LGM of ~0.6 km per 10% precipitation change. Considering the estimates of LGM precipitation change in East Africa (-10% to -30%), we estimate that precipitation can account for ~1 km of glacier length change during the LGM.

DISCUSSION

One of the strengths of using glacier modeling is the ability to explore many possible scenarios of past climate and to identify the similarities and differences between moraine records and independent temperature records, such as the brGDGT records. By forcing the glacier model with independent, brGDGT-based temperature records, we can observe transient evolutions of Rwenzori glaciers and examine whether the simulated glacier fluctuations agree with the moraine record. Below, we explore glacier fluctuations between times of moraine deposition, and we estimate possible ages and climate conditions under which these moraines formed.

Glacier Extents and ELAs during the LGM

It is likely that the Rwenzori glaciers responded to a similar magnitude change in temperature across the mountain range during the LGM. The majority of the discussion focuses on glacier extents in the Bujuku and Mubuku valleys, which drain toward the east, but Osmaston (1989) mapped moraines in multiple valleys, including the Lamya and Nyamugasani valleys, which drain the highlands (Fig. 1). Figure 5A displays simulated glaciers in the Lamya and Nyamugasani valleys reaching the outermost Lake Mahoma stage moraines when the model was forced by a ΔT of -6 °C and ΔP of -10%. These outermost Lake Mahoma stage moraines may also date to the LGM, and future cosmogenic dating would help to inform these speculations.

The results from the SacP-10 and RutP-10 transient simulations indicate that ~6 °C of cooling occurred at high elevations in equatorial East Africa during the LGM. Average LGM conditions (i.e., MeanP-10 and 500yrP-10) did not produce glacier extents near the dated moraines, but simulations that included centennial-scale, high-amplitude temperature changes (i.e., SacP-10 and RutP-10) produced glacier extents close to the dated moraines (Fig. 5A). High-amplitude temperature variability, and particularly cold pulses, would be required if the average cooling at high elevations was ~4.6 °C, as suggested by the average of the two brGDGT temperature reconstructions. The centennial-scale temperature fluctuations in the brGDGT records are generally related to sample-to-sample variability, which some studies

suggest represents "noise" (e.g., Loomis et al., 2017); however, the model results suggest that such centennial-scale variability may be necessary to produce the moraine records if these large temperature fluctuations (as opposed to average LGM temperature conditions) were forcing glacier advances. The simulated glacier length and ELA fluctuations between times of moraine deposition show the potential for rapid glacier advances and retreats. There is no definitive geomorphic evidence for rapid deglaciations in the Bujuku valley during the LGM, but the temperature-sensitive glaciers in the Rwenzori Mountains appear to be capable of rapid changes in these simulations. The large ELA and glacier-length changes during the LGM suggest that the glaciers could have advanced to near their LGM extents and then retreated up-valley of their late glacial extents several times between 31 and 18 ka (Fig. 2).

We also explored the sensitivity of the glaciers to an increase in precipitation during the LGM in two simulations with a ΔP of +30%. Considering the LGM precipitation change in East Africa (-10% to -30%; Shanahan et al., 2008), we estimate that precipitation can account for ~1 km of glacier length change during the LGM, and the remaining ~15.6 km change in length was due to temperature. A steeper lapse rate in the tropics during the LGM would amplify the amount of cooling at high elevations (Porter, 2000; Loomis et al., 2017). We did not alter the lapse rate in these simulations, but future simulations should compare the impact of a change in lapse rate on glacier extent.

The SacP-10 and RutP-10 simulated glaciers approached the locations of undated moraines in multiple valleys during the LGM. The simulated glaciers terminated within the Lake Mahoma stage moraines in the Mubuku valley at 28.5–27.4, 24.5–24.2, and 18.5–15.5 ka (Figs. 2B and 5A). The many undated moraine ridges in the Mubuku valley could correlate to some of these ages, and further dating efforts could reveal a more complete glacial history in this valley.

The simulated LGM ELAs for the Bujuku valley glacier (3720-3750 m asl) were slightly higher than Osmaston's (1989) estimates (3600 m asl) for the same locations (Table S1). This offset is expected because the simulations did not reach the LGM moraines, so the LGM ELA must have been <3720 m asl. The simulated LGM ΔELAs of ~880–850 m are within uncertainty of the tropical average LGM ΔELA of 925 ± 115 m (not accounting for the 120 m decrease in global sea level; Porter, 2000). One possible explanation for the relatively small LGM ΔELA in the Rwenzori Mountains (<650 m) is that Porter (2000) calculated the Lake Mahoma stage ΔELA values using a CE 1955 ELA estimate of 4270 m asl on the east side of the mountain range instead of 4600 m asl as reported by Osmaston (1989). Another possible explanation is that previous studies used ELA estimates from the higher-elevation, undated moraines that were categorized as Lake Mahoma stage (Osmaston, 1989; Porter, 2000; Kaser and Osmaston, 2002; Mark et al., 2005) but appear to be associated with cooling during the late glacial to early Holocene based on the simulations here (Fig. 6A).

Glacier Extents during the Late Glacial

The RutP-10 simulation showed a glacier advance to the high-elevation Lake Mahoma stage moraines at 11.2 ± 0.8 ka (Fig. 6A). It is possible that the high-elevation Lake Mahoma stage moraines near Bigo Bog may be late glacial or early Holocene in age, based on the Lake Rutundu temperature reconstruction and the RutP-10 simulation. This age would imply that the Lake Mahoma stage as mapped by Kaser and Osmaston (2002) might include LGM, late glacial, and Holocene-age moraines, or that these moraines fall within the Omurubaho stage as suggested earlier by Osmaston (1989). The remainder of the Omurubaho stage moraines, which represent glaciers between 4.5 and 7 km in length, are stratigraphically younger than the Lake Mahoma stage moraines, and by inference, should be younger than 12 ka (Fig. 1; Kaser and Osmaston, 2002). Dating these moraines would help clarify the time period and moraine stage to which they belong.

The Sacred Lake and Lake Rutundu records register temperatures that are different from each other during the late glacial period (Loomis et al., 2012, 2017). It is possible that some of this difference is due to the 730 m difference in elevation between the lakes. As discussed above, both the SacP-10 and RutP-10 simulations used a uniform ΔP and, therefore, do not account for arid-humid transitions registered by East African paleoclimate proxy records at 15–14.5 cal k.y. B.P. and 11.5 cal k.y. B.P. (e.g., Roberts et al., 1993; Gasse, 2000) and relatively dry conditions from ca. 13.3 to 11.5 cal k.y. B.P. (e.g., Beuning et al., 1997). While the Rwenzori glaciers are sensitive to changes in temperature, a 20% increase in precipitation could also have contributed toward a glacier advance of ~1 km during the late glacial, based on the simulations.

An interesting question is whether any of the Lake Mahoma stage moraines were deposited during large-scale late glacial climate events, such as the Antarctic Cold Reversal (14.8–12 ka) and/or Younger Dryas (12.7–11.7 ka). The Sacred Lake and Lake Rutundu records do not show cooling during the Antarctic Cold Reversal, but the Lake Rutundu record shows cooling at ca. 12.4 ka, during the Younger Dryas. As mentioned above, the RutP-10 simulation output showed an advance of the Bujuku valley glacier at 11.2 ka reaching a length of 7.4 km due to a ΔT of -4 °C. In this case, the Bujuku valley glacier length reached some mapped Lake Mahoma stage moraines in the upper part of the Bujuku valley. Moraines dating to the Antarctic Cold Reversal are present in the tropical Andes (Jomelli et al., 2014). Further work dating Rwenzori moraines is needed to determine whether there are deposits associated with these late glacial climate events.

Glacier Extents during the Holocene

All Holocene simulations suggested that the Rwenzori glaciers disappeared completely during the early to middle Holocene (Figs. 2 and 3). The simulated glaciers existed with ΔT values <+0.8 °C, but ΔT greater than +0.9 °C (relative to modern

temperatures) mostly caused ice-free conditions. One implication of this result is that the modern Rwenzori glaciers are on the verge of disappearing with even a minor increase (~1 °C) in temperature from modern conditions. Ages from ice cores on Kilimanjaro suggest that ice persisted at 5893 m asl over the past 11.7 k.y. (Thompson et al., 2002). However, these results are at odds with glaciological studies on Kibo (Kilimanjaro's highest peak), which suggest a shorter, discontinuous glacial history during the Holocene (Kaser et al., 2010).

The simulations suggest that the peaks in the Rwenzori Mountains became glacierized within the last 2000 yr. Vegetation and soil development on the Lac Gris stage moraines have been used to infer a deposition age of 0.7–0.1 ka (de Heinzelin, 1953; Osmaston, 1989). The largest late Holocene glacier advances in the simulations occurred at 1.2, 0.8, and 0.7 ka in SacP-10. The times of these advances overlap in age with estimates for the Lac Gris stage moraines (de Heinzelin, 1953; Osmaston, 1989). However, the SacP-10–simulated Bujuku valley glacier extent was ~300 m short of the Lac Gris Stage moraines, suggesting that the climate conditions were slightly cooler. The simulated glacier may have extended farther with a ΔP of 0%, but it is unlikely that regional conditions were much wetter than modern conditions for the past ~1.2 cal k.y. B.P. based on low-elevation records from Lake Edward (Russell et al., 2003).

Tropical Temperatures since the LGM

The Sacred Lake and Lake Rutundu records show a larger LGM cooling than that estimated using general circulation models (Loomis et al., 2017). Rind and Peteet (1985) used a general circulation model and boundary conditions based on CLIMAP LGM temperature estimates and found that, by reducing all CLI-MAP sea-surface temperatures by 2 °C, tropical regions experienced dry and cool conditions (5-6 °C colder than at present) with a corresponding LGM ΔELA of 1000 m (not accounting for a decrease in global sea level). The transient climate simulation, TraCE-21ka, used a synchronously coupled atmosphere-ocean general circulation model in the NCAR-CCSM3 (He, 2011), and the output for East Africa indicated a maximum cooling at 500 hPa (~5500 m asl) of ~5 °C with a slight change in lapse rate. The simulations here (e.g., RutP-10) showed that 6 °C cooling and −10% precipitation change result in a Bujuku valley glacier extent that is ~1.5 km up valley of the LGM target. Based on the glacier model outputs reported here, we suggest that the TraCE-21 simulations underestimate high-elevation temperature change over equatorial East Africa.

East African alpine temperatures respond to global radiative forcing (Chiang, 2009; Loomis et al., 2015) and lapse rate changes (Loomis et al., 2017). Future glacier simulations should include the effects of a steeper lapse rate, which amplified the cooling with elevation in tropical and extratropical locations during the LGM (Farrera et al., 1999; Porter, 2000; Kageyama et al., 2005; Loomis et al., 2017). Lapse rate changes are linked to changes in the tropical hydrological cycle, which, in the East

Africa region, is controlled by moisture transport from the Indian Ocean as well as global atmospheric and oceanic circulation reorganizations, such as changes in the Atlantic Meridional Overturning Circulation (Schefuß et al., 2005; Verschuren et al., 2009; Park and Latif, 2012). For these reasons, we would expect the Rwenzori glaciers and their ELAs to respond to a global climate signal, amplified by a steeper lapse rate during the LGM.

We have shown that the Rwenzori Mountains likely experienced a similar LGM Δ ELA as the rest of the tropics and middle latitudes (e.g., Broecker and Denton, 1990; Porter, 2000). This global shift in climate could have been due to changes in land-ice and sea-ice albedo, water vapor, and cloudiness (Rind and Peteet, 1985) in response to orbital cycles and CO_2 , transferred to the tropics through changes in atmospheric and oceanic circulation (Chiang, 2009; Park and Latif, 2012; Loomis et al., 2015).

CONCLUSIONS

Our six transient simulations of glaciers in the Rwenzori Mountains were driven by brGDGT-based temperature reconstructions from alpine lakes on Mount Kenya over the last 31 k.y. In the results, we see a general agreement between the magnitudes of temperature change from modern conditions in the Mount Kenya records and the magnitude of temperature changes needed to grow the Rwenzori glaciers to near the LGM target (at ~2000 m asl; Osmaston, 1989; Kelly et al., 2014), with the glaciers requiring slightly cooler temperatures (~0.5 °C cooler) to reach the moraines. East African paleoclimate proxy records indicate a reduction in precipitation during the LGM, and, under these conditions, the simulations indicate that temperature changes at high-elevation sites needed to cool by more than 6 °C relative to modern temperatures for the simulated glaciers to reach the LGM target. The simulations suggest LGM ELAs of 3720 m asl and a LGM ΔELA of ~880 m, which is within uncertainty of the tropical average (LGM ΔELA 925 ± 115 m; Porter, 2000).

One simulation (RutP-10) suggests that some of the moraines at ~ 3500 m asl in the Bujuku valley could have been deposited during the late glacial or early Holocene ca. 11.2 ka. The simulations show ice-free conditions during the majority of the early and middle Holocene, and ice-free conditions could occur in the near future in the Rwenzori with a warming of ~ 1 °C from modern temperatures. The simulations indicate that the Rwenzori peaks became glacierized within the last 2000 yr. Increased efforts in cosmogenic dating in the future will help to inform these simulated predictions.

ACKNOWLEDGMENTS

We thank the Neukom Institute at Dartmouth College, and acknowledge grants from the National Science Foundation (EAR-1702319 and 1702293), the Comer Science and Education Foundation (CP103 and GSSF13), and the National Geographic Society (8886-11) for funding. We thank S. Loomis

for access to the published branched glycerol dialkyl glycerol tetraether (brGDGT) temperature data. We are grateful for field assistance by Rwenzori Trekking Services and Rwenzori Mountaineering Services, and the support of the Ugandan Wildlife Authority and the Ugandan National Council on Science and Technology (research permit numbers UWA/TDO/33/02, NS395, and Material Transfer Agreement 151).

REFERENCES CITED

- Anderson, B., Mackintosh, A., Stumm, D., George, L., Kerr, T., Winter-Billington, A., and Fitzsimons, S., 2010, Climate sensitivity of a high-precipitation glacier in New Zealand: Journal of Glaciology, v. 56, p. 114–128, https://doi.org/10.3189/002214310791190929.
- Benn, D.I., Owen, L.A., Osmaston, H.A., Seltzer, G.O., Porter, S.C., and Mark, B., 2005, Reconstruction of equilibrium-line altitudes for tropical and sub-tropical glaciers: Quaternary International, v. 138–139, p. 8–21, https://doi.org/10.1016/j.quaint.2005.02.003.
- Berke, M.A., Johnson, T.C., Werne, J.P., Livingstone, D.A., Grice, K., Schouten, S., and Sinningha Damste, J.S., 2014, Characterization of the last deglacial transition in tropical East Africa: Insights from Lake Albert: Palaeogeography, Palaeoclimatology, Palaeoecology, v. 409, p. 1–8, https://doi.org/10.1016/j.palaeo.2014.04.014.
- Beuning, K.R.M., Talbot, M.R., and Kelts, K., 1997, A revised 30,000-year paleoclimatic and paleohydrologic history of Lake Albert, East Africa: Palaeogeography, Palaeoclimatology, Palaeoecology, v. 136, p. 259–279, https://doi.org/10.1016/S0031-0182(97)00034-5.
- Bonnefille, R., Roeland, J.C., and Guiot, J., 1990, Temperature and rainfall estimates for the past 40,000 years in equatorial Africa: Nature, v. 346, p. 347–349, https://doi.org/10.1038/346347a0.
- Briner, J.P., and Kaufman, D.S., 2008, Late Pleistocene mountain glaciation in Alaska: Key chronologies: Journal of Quaternary Science, v. 23, p. 659–670, https://doi.org/10.1002/jqs.1196.
- Briner, J.P., Kaufman, D.S., Manley, W.F., Finkel, R.C., and Caffee, M.W., 2005, Cosmogenic exposure dating of late Pleistocene moraine stabilization in Alaska: Geological Society of America Bulletin, v. 117, p. 1108– 1120, https://doi.org/10.1130/B25649.1.
- Broecker, W.S., and Denton, G.H., 1990, The role of ocean-atmosphere reorganizations in glacial cycles: Quaternary Science Reviews, v. 9, p. 305–341, https://doi.org/10.1016/0277-3791(90)90026-7.
- Bromley, G.R.M., Hall, B.L., Schaefer, J.M., Winckler, G., Todd, C.E., and Rademaker, K.M., 2011, Glacier fluctuations in the southern Peruvian Andes during the late-glacial period, constrained with cosmogenic ³He: Journal of Quaternary Science, v. 26, p. 37–43, https://doi.org/10.1002/jqs.1424.
- Bromley, G.R.M., Schaefer, J.M., Hall, B.L., Rademaker, K.M., Putnam, A.E., Todd, C.E., Hegland, M., Winckler, G., Jackson, M.S., and Strand, P.D., 2016, A cosmogenic ¹⁰Be chronology for the local Last Glacial Maximum and termination in the Cordillera Oriental, southern Peruvian Andes: Implications for the tropical role in global climate: Quaternary Science Reviews, v. 148, p. 54–67, https://doi.org/10.1016/j.quascirev 2016.07.010
- Chiang, J.C.H., 2009, The tropics in paleoclimate: Annual Review of Earth and Planetary Sciences, v. 37, p. 263–297, https://doi.org/10.1146/annurev.earth.031208.100217.
- Clark, P.U., Dyke, A.S., Shakun, J.D., Carlson, A.E., Clark, J., Wolhfarth, B., Mitrovica, J.X., Hostetler, S.W., and McCabe, A.M., 2009, The Last Glacial Maximum: Science, v. 325, p. 710–714, https://doi.org/10.1126/ science.1172873.
- de Heinzelin, J., 1953, Les stades de recession du glacier Stanley occidental: Exploration du Parc National des Virunga (Parc National Albert), Brussels, Institut des Parcs Nationaux du Congo Belge, 25 p.
- Doughty, A.M., Anderson, B.M., Mackintosh, A.N., Kaplan, M.R., Vandergoes, M.J., Barrell, D.J.A., Denton, G.H., Schaefer, J.M., Chinn, T.J.H., and Putnam, A.E., 2013, Evaluation of Lateglacial temperatures in the Southern Alps of New Zealand based on glacier modelling at Irishman Stream, Ben Ohau Range: Quaternary Science Reviews, v. 74, p. 160–169, https://doi.org/10.1016/j.quascirev.2012.09.013.

- Doughty, A.M., Schaefer, J.M., Putnam, A.E., Denton, G.H., Kaplan, M.R., Barrell, D.J.A., Anderson, B.G., Kelley, S.E., Finkel, R.C., and Schwartz, R., 2015, Mismatch of glacier extent and summer insolation in Southern Hemisphere mid-latitudes: Geology, v. 43, p. 407–410, https://doi. org/10.1130/G36477.1.
- Doughty, A.M., Mackintosh, A.N., Anderson, B.M., Dadic, R., Putnam, A.E., Barrell, D.J.A., Denton, G.H., Chinn, T.J.H., and Schaefer, J.M., 2017, An exercise in glacier length modeling: Interannual climatic variability alone cannot explain Holocene glacier fluctuations in New Zealand: Earth and Planetary Science Letters, v. 470, p. 48–53, https://doi.org/10.1016/j .epsl.2017.04.032.
- Farber, D.L., Hancock, G.S., Finkel, R.C., and Rodbell, D.T., 2005, The age and extent of tropical alpine glaciation in the Cordillera Blanca, Peru: Journal of Quaternary Science, v. 20, p. 759–776, https://doi.org/10.1002/jqs.994.
- Farrera, I., Harrison, S.P., Prentice, I.C., Ramstein, G., Guiot, J., Bartlein, P.J., Bonnefille, R., Bush, M., Cramer, W., von Grafenstein, U., Holmgren, K., Hooghiemstra, H., Hope, G., Jolly, D., Lauritzen, S.-E., Ono, Y., Pinot, S., Stute, M., and Yu, G., 1999, Tropical climates at the Last Glacial Maximum: A new synthesis of terrestrial palaeoclimate data. I. Vegetation, lake-levels and geochemistry: Climate Dynamics, v. 15, p. 823–856, https://doi.org/10.1007/s003820050317.
- Gasse, F., 2000, Hydrological changes in the African tropics since the Last Glacial Maximum: Quaternary Science Reviews, v. 19, p. 189–211, https://doi.org/10.1016/S0277-3791(99)00061-X.
- Gosse, J.C., Evenson, E.B., Klein, J., Lawn, B., and Middleton, R., 1995, Precise cosmogenic ¹⁰Be measurements in western North America: Support for a global Younger Dryas cooling event: Geology, v. 23, p. 877–880, https://doi.org/10.1130/0091-7613(1995)023<0877:PCBMIW>2.3 .CO:2.
- Haberyan, K.A., and Hecky, R.E., 1987, The late Pleistocene and Holocene stratigraphy and paleolimnology of Lakes Kivu and Tanganyika: Palaeogeography, Palaeoclimatology, Palaeoecology, v. 61, p. 169–197, https:// doi.org/10.1016/0031-0182(87)90048-4.
- He, F., 2011, Simulating Transient Climate Evolution of the Last Deglaciation with CCSM3 [Ph.D. thesis]: Madison, Wisconsin, University of Wisconsin–Madison, 185 p.
- Jarvis, A., Reuter, H.I., Nelson, A., and Guevara, E., 2008, Hole-filled SRTM for the Globe, Version 4: available from the Consultative Group on International Agricultural Research Consortium for Spatial Information (CGIAR-CSI) Shuttle Radar Topography Mission (SRTM) 90 m Digital Elevation Database, http://srtm.csi.cgiar.org (accessed 2014).
- Jomelli, V., Favier, V., Vuille, M., Braucher, R., Martin, L., Blard, P.-H., Colose, C., Brunstein, D., He, F., Khodri, M., Bourles, D.L., Leanni, L., Rinter-knecht, V., Grancher, D., Francou, B., Ceballos, J.L., Fonseca, H., Liu, Z., and Otto-Bliesner, B.L., 2014, A major advance of tropical Andean glaciers during the Antarctic Cold Reversal: Nature, v. 513, p. 224–228, https://doi.org/10.1038/nature13546.
- Kageyama, M., Harrison, S.P., and Abe-Ouchi, A., 2005, The depression of tropical snowlines at the Last Glacial Maximum: What can we learn from climate model experiments?: Quaternary International, v. 138–139, p. 202–219, https://doi.org/10.1016/j.quaint.2005.02.013.
- Kaplan, M.R., Schaefer, J.M., Denton, G.H., Barrell, D.J.A., Chinn, T.J.H., Putnam, A.E., Andersen, B.G., Finkel, R.C., Schwartz, R., and Doughty, A.M., 2010, Glacier retreat in New Zealand during the Younger Dryas stadial: Nature, v. 467, p. 194–197, https://doi.org/10.1038/nature09313.
- Kaplan, M.R., Schaefer, J.M., Denton, G.H., Doughty, A.M., Barrell, D.J.A., Chinn, T.J.H., Putnam, A.E., Andersen, B.G., Mackintosh, A., Finkel, R.C., Schwartz, R., and Anderson, B., 2013, The anatomy of long-term warming since 15 ka in New Zealand based on net glacier snowline rise: Geology, v. 41, p. 887–890, https://doi.org/10.1130/G34288.1.
- Kaser, G., 2001, Glacier-climate interaction at low latitudes: Journal of Glaciology, v. 47, p. 195–204, https://doi.org/10.3189/172756501781832296.
- Kaser, G., and Osmaston, H., 2002, Tropical Glaciers: Cambridge, UK, Cambridge University Press, 207 p.
- Kaser, G., Molg, T., Cullen, N.J., Hardy, D.R., and Winkler, M., 2010, Is the decline of ice on Kilimanjaro unprecedented in the Holocene?: The Holocene, v. 20, p. 1079–1091, https://doi.org/10.1177/0959683610369498.
- Kaufmann, G., and Romanov, D., 2012, Landscape evolution and glaciation of the Rwenzori Mountains, Uganda: Insights from numerical modeling: Geomorphology, v. 138, no. 1, p. 263–275, https://doi.org/10.1016/j .geomorph.2011.09.011.

- Kelley, S.E., Kaplan, M.R., Schaefer, J.M., Andersen, B.G., Barrell, D.J.A., Putnam, A.E., Denton, G.H., Schwartz, R., Finkel, R.C., and Doughty, A.M., 2014, New Zealand moraine record of a Southern Hemisphere cold episode 41,000 years ago: Earth and Planetary Science Letters, v. 405, p. 194–206, https://doi.org/10.1016/j.epsl.2014.07.031.
- Kelly, M.A., Lowell, T.V., Applegate, P.J., Smith, C.A., Phillips, F.M., and Hudson, A.M., 2012, Late glacial fluctuations of Quelccaya ice cap, southeastern Peru: Geology, v. 40, p. 991–994, https://doi.org/10.1130/G33430.1.
- Kelly, M.A., Russell, J.M., Baber, M.B., Howley, J.A., Loomis, S.E., Zimmerman, S., Nakileza, B., and Lukaye, J., 2014, Expanded glaciers during a dry and cold Last Glacial Maximum in equatorial East Africa: Geology, v. 42, p. 519–522, https://doi.org/10.1130/G35421.1.
- Kessler, M.A., Anderson, R.S., and Stock, G.M., 2006, Modeling topographic and climatic control of east-west asymmetry in Sierra Nevada glacier length during the Last Glacial Maximum: Journal of Geophysical Research, v. 111, F02002, https://doi.org/10.1029/2005JF000365.
- Le Meur, E., Gagliardini, O., Zwinger, T., and Ruokolainen, J., 2004, Glacier flow modelling: A comparison of the Shallow Ice Approximation and the full-Stokes solution: Comptes Rendus Physique, v. 5, no. 7, p. 709–722, https://doi.org/10.1016/j.crhy.2004.10.001.
- Lentini, G., Cristofanelli, P., Duchi, R., Marinoni, A., Verza, G., Vuillermoz, E., Toffolon, R., and Bonasoni, P., 2011, Mount Rwenzori (4750 m a.s.l., Uganda): Meteorological characterization and air-mass transport analysis: Geografia Fisica e Dinamica Quaternaria, v. 34, no. 3, p. 183–193.
- Licciardi, J.M., and Pierce, K.L., 2008, Cosmogenic exposure–age chronologies of Pinedale and Bull Lake glaciations in greater Yellowstone and the Teton Range, USA: Quaternary Science Reviews, v. 27, no. 7–8, p. 814–831, https://doi.org/10.1016/j.quascirev.2007.12.005.
- Livingstone, D.A., 1967, Postglacial vegetation of the Ruwenzori Mountains in equatorial Africa: Ecological Monographs, v. 37, p. 25–52, https://doi.org/10.2307/1948481.
- Loomis, S.E., Russell, J.M., Ladd, B., Street-Perrott, F.A., and Sinninghe-Damste, J.S., 2012, Calibration and application of the branched GDGT temperature proxy on East African lake sediments: Earth and Planetary Science Letters, v. 357–358, p. 277–288, https://doi.org/10.1016/j.epsl .2012.09.031.
- Loomis, S.E., Russell, J.M., and Lamb, H.F., 2015, Northeast African temperature variability since the late Pleistocene: Palaeogeography, Palaeoclimatology, Palaeoecology, v. 423, p. 80–90, https://doi.org/10.1016/j.palaeo.2015.02.005.
- Loomis, S.E., Russell, J.M., Verschuren, D., Morill, C., De Cort, G., Sinninghe Damsté, J.S., Olago, D., Eggermont, H., Street-Perrott, F.A., and Kelly, M.A., 2017, The tropical lapse rate steepened during the Last Glacial Maximum: Science Advances, v. 3, p. e1600815, https://doi.org/10.1126/sciadv.1600815.
- Marchetti, D.W., Cerling, T.E., and Lips, E.W., 2005, A glacial chronology for the Fish Creek drainage of Boulder Mountain, Utah, USA: Quaternary Research, v. 64, no. 2, p. 264–271, https://doi.org/10.1016/j.yqres .2005.05.004.
- Mark, B.G., Harrison, S.P., Spessa, A., New, M., Evans, D.J.A., and Helmens, K.F., 2005, Tropical snowline changes at the Last Glacial Maximum: A global assessment: Quaternary International, v. 138–139, p. 168–201, https://doi.org/10.1016/j.quaint.2005.02.012.
- Mizuno, K., 1998, Succession processes of alpine vegetation in response to glacial fluctuations of Tyndall Glacier, Mt. Kenya, Kenya: Arctic and Alpine Research, v. 30, p. 340–348, https://doi.org/10.2307/1552006.
- Mölg, T., Cullen, N.J., Hardy, D.R., Kaser, G., and Klok, L., 2008, Mass balance of a slope glacier on Kilimanjaro and its sensitivity to climate: Journal of Climatology, v. 28, p. 881–892, https://doi.org/10.1002/joc.1589.
- New, M., Lister, D., Hulme, M., and Makin, I., 2002, A high-resolution data set of surface climate over global land areas: Climate Research, v. 21, p. 1–25, https://doi.org/10.3354/cr021001.
- Oerlemans, J., 1992, Climate sensitivity of glaciers in southern Norway: Application of an energy-balance model to Nigardsbreen, Hellstugubreen and Alfotbreen: Journal of Glaciology, v. 38, p. 223–232, https://doi.org/10.1017/S0022143000003634.
- Oerlemans, J., 2001, Glaciers and Climate Change: Rotterdam, Netherlands, A.A. Balkema Publishers, 148 p.
- Osmaston, H., 1989, Glaciers, glaciations and equilibrium line altitudes on the Rwenzori, *in* Mahaney, W.C., ed., Quaternary and Environmental Research on East African Mountains: Rotterdam, Netherlands, A.A. Balkema Publishers, p. 31–104.

- Osmaston, H., 2004, Quaternary glaciations in the East African mountains, *in* Ehlers, J., and Gibbard, P.L., eds., Quaternary Glaciations—Extent and Chronology, Part III: South America, Asia, Africa, Australia, Antarctic: Amsterdam, Elsevier, p. 139–150.
- Osmaston, H.A., and Harrison, S.P., 2005, The late Quaternary glaciation of Africa: A regional synthesis: Quaternary International, v. 138–139, p. 32–54, https://doi.org/10.1016/j.quaint.2005.02.005.
- Otto-Bliesner, B.L., Russell, J.M., Clark, P.U., Liu, Z., Overpeck, J.T., Konecky, B., deMenocal, P., Nicholson, S.E., He, F., and Lu, Z., 2014, Coherent changes of southeastern equatorial and northern African rainfall during the last deglaciation: Science, v. 346, p. 1223–1227, https://doi.org/10.1126/science.1259531.
- Park, W., and Latif, M., 2012, Atlantic Meridional Overturning Circulation response to idealized external forcing: Climate Dynamics, v. 39, p. 1709– 1726, https://doi.org/10.1007/s00382-011-1212-0.
- Plummer, M.A., and Phillips, F.M., 2003, A 2-D numerical model of snow/ ice energy balance and ice flow for paleoclimatic interpretation of glacial geomorphic features: Quaternary Science Reviews, v. 22, p. 1389–1406, https://doi.org/10.1016/S0277-3791(03)00081-7.
- Porter, S.C., 1975, Equilibrium-line altitudes of late Quaternary glaciers in the Southern Alps, New Zealand: Quaternary Research, v. 5, p. 27–47, https://doi.org/10.1016/0033-5894(75)90047-2.
- Porter, S.C., 2000, Snowline depression in the tropics during the last glaciation: Quaternary Science Reviews, v. 20, p. 1067–1091, https://doi.org/10.1016/S0277-3791(00)00178-5.
- Putnam, A.E., Schaefer, J.M., Barrell, D.J.A., Vandergoes, M., Denton, G.H., Kaplan, M.R., Schwartz, R., Finkel, R.C., Goehring, B.M., and Kelley, S.E., 2010, In situ cosmogenic ¹⁰Be production-rate calibration from the Southern Alps, New Zealand: Quaternary Geochronology, v. 5, p. 392–409, https://doi.org/10.1016/j.quageo.2009.12.001.
- Putnam, A.E., Schaefer, J.M., Denton, G.H., Barrell, D.J.A., Birkel, S.D., Andersen, B.G., Kaplan, M.R., Finkel, R.C., Schwartz, R., and Doughty, A.M., 2013, The Last Glacial Maximum at 44°S documented by a ¹⁰Be moraine chronology at Lake Ohau, Southern Alps of New Zealand: Quaternary Science Reviews, v. 62, p. 114–141, https://doi.org/10.1016/j.quascirev.2012.10.034.
- Rind, D., and Peteet, D., 1985, Terrestrial conditions at the Last Glacial Maximum and CLIMAP sea-surface temperature estimates: Are they consistent?: Quaternary Research, v. 24, p. 1–22, https://doi.org/10.1016/0033 -5894(85)90080-8.
- Roberts, N., Taieb, M., Barker, P., Damnati, B., Icole, M., and Williamson, D., 1993, Timing of the Younger Dryas event in East Africa from lake-level changes: Nature, v. 366, p. 146–148, https://doi.org/10.1038/366146a0.
- Røhr, P.C., and Killingtveit, Å., 2003, Rainfall distribution on the slopes of Mt. Kilimanjaro: Hydrological Sciences Journal, v. 48, p. 65–77, https://doi.org/10.1623/hysj.48.1.65.43483.
- Russell, J.M., Johnson, T.C., and Talbot, M.R., 2003, A 725 yr cycle in the climate of central Africa during the late Holocene: Geology, v. 31, p. 677– 680, https://doi.org/10.1130/G19449.1.
- Sagredo, E.A., Rupper, S., and Lowell, T.V., 2014, Sensitivities of the equilibrium line altitude to temperature and precipitation changes along the Andes: Quaternary Research, v. 81, p. 355–366, https://doi.org/10.1016/j.yqres.2014.01.008.
- Sagredo, E.A., Kaplan, M.R., Araya, P.S., Lowell, T.V., Aravena, J.C., Moreno, P.I., Kelly, M.A., and Schaefer, J.M., 2018, Trans-Pacific glacial response to the Antarctic Cold Reversal in the southern mid-latitudes: Quaternary Science Reviews, v. 188, p. 160–166, https://doi.org/10.1016/j.quascirev .2018.01.011.
- Schaefer, J.M., Denton, G.H., Barrell, D.J.A., Ivy-Ochs, S., Kubik, P.W., Andersen, B.G., Phillips, F.M., Lowell, T.V., and Schluchter, C., 2006, Near-synchronous interhemispheric termination of the Last Glacial Maximum in mid-latitudes: Science, v. 312, no. 5779, p. 1510–1513, https://doi.org/10.1126/science.1122872.
- Schaefer, J.M., Denton, G.H., Kaplan, M., Putnam, A., Finkel, R.C., Barrell, D.J.A., Andersen, B.G., Schwartz, R., Mackintosh, A., Chinn, T., and Schlüchter, C., 2009, High-frequency Holocene glacier fluctuations in New Zealand differ from the northern signature: Science, v. 324, p. 622–625, https://doi.org/10.1126/science.1169312.
- Schefuß, E., Schouten, S., and Schneider, R.R., 2005, Climate controls on central African hydrology during the past 20,000 years: Nature, v. 437, p. 1003–1006, https://doi.org/10.1038/nature03945.

- Shanahan, T.M., and Zreda, M., 2000, Chronology of Quaternary glaciations in East Africa: Earth and Planetary Science Letters, v. 177, p. 23–42, https:// doi.org/10.1016/S0012-821X(00)00029-7.
- Shanahan, T.M., Overpeck, J.T., Scholz, C.A., Beck, J.W., Peck, J., and King, J.W., 2008, Abrupt changes in the water balance of tropical West Africa during the late Quaternary: Journal of Geophysical Research, v. 113, D12108, https://doi.org/10.1029/2007JD009320.
- Stager, J.C., Ryves, D.B., Chase, B.M., and Pausata, F.S.R., 2011, Catastrophic drought in the Afro-Asian monsoon during Heinrich event 1: Science, v. 331, p. 1299–1302, https://doi.org/10.1126/science.1198322.
- Stroup, J.S., Kelly, M.A., Lowell, T.V., Applegate, P.J., and Howley, J.A., 2014, Late Holocene fluctuations of Qori Kalis outlet glacier, Quelccaya ice cap, Peruvian Andes: Geology, v. 42, p. 347–350, https://doi.org/10.1130/ G35245.1.
- Talbot, M.R., and Livingstone, D.A., 1989, Hydrogen index and carbon isotopes of lacustrine organic matter as lake level indicators: Palaeogeography, Palaeoclimatology, Palaeoecology, v. 70, p. 121–137, https://doi.org/10.1016/0031-0182(89)90084-9.
- Taylor, R.G., Mileham, L., Tindimugaya, C., Majugu, A., Muwanga, A., and Nakileza, B., 2006, Recent glacial recession in the Rwenzori Mountains of East Africa due to rising air temperature: Geophysical Research Letters, v. 33, L10402, https://doi.org/10.1029/2006GL025962.
- Thackray, G.D., Lundeen, K.A., and Borgert, J.A., 2004, Latest Pleistocene alpine glacier advances in the Sawtooth Mountains, Idaho, USA: Reflections of midlatitude moisture transport at the close of the last glaciation: Geology, v. 32, no. 3, p. 225–228, https://doi.org/10.1130/G20174.1.
- Thompson, L.G., Mosley-Thompson, E., Davis, M.E., Henderson, K.A., Brecher, H.H., Zagorodnov, V.S., Mashiotta, T.A., Lin, P.-N., Mikhalenko, V.N., Hardy, D.R., and Beer, J., 2002, Kilimanjaro ice core records:

- Evidence of Holocene climate change in tropical Africa: Science, v. 298, p. 589–593, https://doi.org/10.1126/science.1073198.
- Tierney, J.E., Russell, J.M., Huang, Y., Sinninghe Damste, J.S., Hopmans, E.C., and Cohen, A.S., 2008, Northern Hemisphere controls on tropical southeast African climate during the past 60,000 years: Science, v. 322, p. 252–255, https://doi.org/10.1126/science.1160485.
- Verschuren, D., Sinninghe Damste, J.S., Moernaut, J., Kristen, I., Blaauw, M., Fagot, M., Haug, G.H., and CHALLACEA Project members, 2009, Halfprecessional dynamics of monsoon rainfall near the East African equator: Nature, v. 462, p. 637–641, https://doi.org/10.1038/nature08520.
- Walker, M.J.C., Berkelhammer, M., Bjorck, S., Cwynar, L.C., Fisher, D.A., Long, A.J., Lowe, J.J., Newnham, R.M., Rasmussen, S.O., and Weiss, H., 2012, Formal subdivision of the Holocene Series/Epoch: A discussion paper by a working group of INTIMATE (Integration of Ice-Core, Marine and Terrestrial Records) and the Subcommission on Quaternary Stratigraphy (International Commission on Stratigraphy): Journal of Quaternary Science, v. 27, p. 649–659, https://doi.org/10.1002/jqs.2565.
- Xu, X., Wang, L., and Yang, J., 2010, Last Glacial Maximum climate inferences from integrated reconstruction of glacier equilibrium-line altitude for the head of the Urumqi River, Tianshan Mountains: Quaternary International, v. 218, p. 3–12, https://doi.org/10.1016/j.quaint.2009.11.027.
- Zech, R., Zech, M., Kubik, P.W., Kharki, K., and Zech, W., 2009, Deglaciation and landscape history around Annapurna, Nepal, based on ¹⁰Be surface exposure dating: Quaternary Science Reviews, v. 28, p. 1106–1118, https://doi.org/10.1016/j.quascirev.2008.11.013.

Manuscript Accepted by the Society 23 December 2019